



Glass gilding process in medieval Syria and Egypt (13th–14th century)

Eléonore Gueit^{a,b,*}, Evelyne Darque-Ceretti^a, Marc Aucouturier^b

^a MINES Paristech, CEMEF – Centre de Mise en Forme des Matériaux, CNRS UMR 7635, BP 207, 06904 Sophia-Antipolis cedex, France

^b Centre de Recherche et de Restauration des Musées de France, C2RMF (CNRS UMR 171), Palais du Louvre, Porte des Lions, 75001 Paris, France

ARTICLE INFO

Article history:

Received 16 February 2009

Received in revised form

21 August 2009

Accepted 31 August 2009

Keywords:

Islamic art

Glass

Enamel

Gold

Interface

Adhesion

Diffusion

ABSTRACT

Twelve gilded and enamelled Islamic glass fragments, produced in Syria or Egypt during the Ayyubid or Mamluk period, were provided by the Louvre museum for complete non-destructive analysis. The enamelling process of similar objects has been extensively studied in the last decades, but the gilding process has never been investigated in details. This paper focuses on the understanding of both the gilding process and the gold/glass adhesion mechanism. The structure, composition and thickness of the gold flakes forming the gilding decoration are measured. The complete process combining gilding and enamelling is described and the local mechanism of adhesion of gold flakes on the glass body is discussed.

© 2010 Elsevier Ltd. All rights reserved.

1. Introduction

Enamelled and gilded glass is one of the most outstanding artistic productions of the Islamic craft industry, especially during the Ayyubid and Mamluk dynasties (Syria and Egypt, 13th and 14th centuries) (Lamm, 1941). Islamic glassware was already widely distributed in the western world, but the scientific interest for Islamic glass production only started in the middle of the 19th century. The first studies were devoted to iconographic and stylistic aspects only (d'Avennes, 1877; Schmoranz, 1899). Scientific and technical investigations became possible with the emergence of non-destructive analysis methods, and gilded and enamelled objects have been extensively studied in the last decades. Two major publications (Carboni and Whitehouse, 2001; Ward, 1998) provide what may be considered as the most complete state-of-the-art of the current knowledge about fabrication techniques and materials as well as production centres and their trade diffusion. A large number of data is available on the composition and structure of both glass bodies and decorative enamels (Freestone and Stapleton, 1998; Freestone, 2002; Henderson, 1998; Verità,

1998). However, the enamelling process is not fully understood. In particular the temperatures and number of firing remain vaguely described.

The gilding process is rarely mentioned in the literature. Authors who mention it all admit that gold is ground into powder, mixed with a binder of gum Arabic kind and applied with a brush before firing (Carboni, 2001a; Gudenrath, 2001; du Pasquier, 2005). Also in ancient sources the descriptions of this specific glass gilding process are very rare or non-existent. The Abu'l Quasim treatise, written in 1301, (Allan, 1973) describes in detail the gilding of Islamic ceramics with gold foils but does not mention glass gilding process. A gold painting technique is described in the 12th century treatise by Théophilus (2000). That treatise refers to Byzantine techniques anterior to the Mamelouk period, but the Syrian glassmakers worked in the same tradition as the Byzantine artists.

This paper describes the result of a comprehensive laboratory study of 12 gilded and enamelled glassware fragments kindly selected and provided by the Department of Islamic Art of the Louvre museum. On the archaeological point of view, the purpose of this study is the understanding of the gilding technique: What tools and materials were used by the artisans? How was gold applied to the glass surface? Are there similarities between the glass and the ceramic productions?

On the scientific point of view, this paper brings new information on the adhesion mechanisms between gold and glass, which is a difficult and unsolved issue. Some publications recently offered

* Corresponding author. MINES Paristech, CEMEF – Centre de Mise en Forme des Matériaux, CNRS UMR 7635, BP 207, 06904 Sophia-Antipolis cedex, France.

E-mail addresses: eleonore.gueit@mines-paristech.fr (E. Gueit), Evelyne.Darque-Ceretti@mines-paristech.fr (E. Darque-Ceretti), Marc.Aucouturier@culture.gouv.fr (M. Aucouturier).

physical models of the adhesion mechanism in very specific cases (Darque-Ceretti et al., 2002, 2008), but the question of adhesion between glass and ground gold was never considered.

2. Materials and techniques

2.1. Studied fragments

Twelve fragments were chosen amongst the collection of the Department of Islamic Arts of the Louvre museum, in agreement with the curator in chief, as representative of the production of gilded and enamelled glassware during the Ayyubid and Mamluk period (Syria and Egypt 13th–14th century) (Fig. 1). They cover all the range of enamel colours existing in that collection, except yellow. Most of them show typical dark-red enamelled lines surrounding enamels and gilded patterns. Two fragments made of coloured glass were chosen in order to identify the colouring agent and identify possible differences in composition with the uncoloured fragments. The fragments are in variable conservation state. Some fragments are in an excellent state, others are whitened or strongly weathered. Some gilded decorations are very dense and shining, others show large gaps.

2.2. Experimental techniques

Because of the cultural heritage value of the fragments, no sampling was allowed and the study had to be entirely conducted by non-invasive methods. The recent development of non-destructive analysis methods now allows obtaining very rich information on cultural heritage objects (Darque-Ceretti and Aucouturier, 2007).

First the objects were carefully observed by optical microscopy (binocular microscope) in both reflected and transmitted light.

Thanks to their limited size, they could be inserted into the chamber of a scanning electron microscope (SEM, Philips XL30CP), operated at 20 kV acceleration voltage and under limited vacuum (100 Pa) to avoid charging effects. In such a limited vacuum configuration, the magnification is limited to about $\times 1000$.

As no sampling was allowed, it was impossible to observe cross-sections. For most of the samples the observations were made on the surface only. Fortunately two fragments showed a very clean broken edge that could be observed without preparation.

An X-ray energy dispersive spectrometry (EDS) attachment allowed local microanalysis. In limited vacuum configuration, SEM-EDS microanalysis may be affected by the so-called “skirting effect”



Fig. 1. images of the studied objects. Egypt or Syria, 13th or 14th century. Musée du Louvre, Department of Islamic art. Photographs © C2RMF, D. Bagault. **“waq-waq” is a legendary tree whose fruits in shape of animal heads say “waq-waq” when they are gathered.

(Carlton et al., 2004): electrons from the incident beam are elastically scattered by the residual gas and hit the specimen far from the actual beam impact. Collected X-rays may thus be issued from an area much larger than the actual beam spot and the corresponding emission volume. For very heterogeneous surfaces the results might be distorted.

The objects were submitted to ion beam microanalysis (IBA) to obtain more precise local analysis than with EDS measurements, using the particle accelerator AGLAE available in the Centre de Recherche et de Restauration des Musées de France (C2RMF). AGLAE is equipped with an extracted micro-beam allowing direct non-destructive analysis of the objects in free atmosphere (Calligaro et al., 2004). It offers the possibility to use PIXE (Particle Induced X-ray Emission) and PIGE (Particle Induced Gamma-ray Emission), which provides the elementary composition at the point of analysis to a depth of a few micrometers, and RBS (Rutherford Backscattering Spectrometry), which measures in-depth profiles of the major elements. The diameter of the beam is around 50 μm . PIXE results are quantified using GUPIX code (Maxwell et al., 1988). RBS spectra are simulated by the SIMNRA code (Mayer, 1997), which describes the analysed depth as a succession of discrete layers with adjustable composition and thickness.

Raman micro spectrometry measurements were necessary to confirm the nature of the pigments used in some enamels. The equipment used is a confocal Jobin-Yvon Labram Infinity, with 532 and 633 nm lasers, a notch filter and $\times 50$ or $\times 100$ objectives (lateral resolution around 2 μm).

Micro topography measurements of the surface roughness were performed using a STIL CHR 150 instrument, based on spectrometric analysis of the light reflected by the surface under white illumination (confocal microscopy by chromating coding in extended field) (Ezrati et al., 2007). The configuration used in the present investigation (illumination spot 10 μm , collection step 3 μm) allows a lateral resolution of 1 μm and a height resolution of 100 nm.

3. Results

3.1. Glass and enamels

Although the object of the study is not the enamelling process itself, the glass and enamels compositions were systematically measured to make sure they were coherent with the literature and to collect all necessary data to understand the gold/glass interface.

3.1.1. Glass bodies

The average glass compositions obtained by PIXE measurements under 3 MeV protons are summarised in Table 1; all glasses are soda-lime glasses. The Na_2O content is lower than expected because of the well known phenomenon of surface weathering. Indeed PIXE analysis gives the sodium concentration of the first micrometer of the surface only (absorption depth of the Na $K\alpha$ X-ray emission). When using PIGE analysis, the analysed depth is much larger (several tens of μm (Tesmer and Nastasi, 1995)). The analysed volume is not weathered and is richer in sodium than the first microns of the surface. The sodium oxide content found by PIGE analysis (Table 1) is between 8 and 13 wt%. The obtained values are in general agreement with the literature on ancient glass (Brill, 2001; Carboni, 2003; Freestone and Stapleton, 1998; Verità, 1998), considering that analyses methods are different and specimens may have been submitted to different weathering and conservation conditions. This surface alteration of the glass can be quantified by RBS analysis. Fig. 2 shows examples of the surface morphology of an altered fragment and of a simulated RBS

Table 1

Average composition and error margin 1 sigma in wt% of the glass bodies, compared to literature data (Freestone and Stapleton, 1998; Verità, 1998).

Analysis method	Present study	Freestone, 1998	Verità, 1998
	PIXE (all elements) PIGE (Na)	SEM-EDS	SEM-EDS
SiO_2	69 \pm 4.1	69 \pm 2.1	68.9 \pm 2.8
Na_2O	10.5 \pm 2.9	13.3 \pm 1.8	11.7 \pm 1.1
MgO	1.7 \pm 2.2	2.9 \pm 1.5	3.4 \pm 0.5
Al_2O_3	1.6 \pm 1	1.1 \pm 0.4	1.1 \pm 0.5
K_2O	2.8 \pm 0.8	3.0 \pm 1.6	2.5 \pm 0.6
CaO	7 \pm 3	7.5 \pm 2.2	7.9 \pm 1.5
Fe_2O_3	0.7 \pm 0.2	0.5 \pm 0.3	0.4 \pm 0.1
MnO	1.4 \pm 0.7 Except MAO 490/40: 5.1	1.2 \pm 0.7	1.2 \pm 0.4
Cl	1.2 \pm 0.7	0.8 \pm 0.2	0.7 \pm 0.05

spectrum on another one. The simulation of the RBS spectrum is obtained by adding on the top of the glass with normal composition a surface layer of about 0.4 μm thickness containing no sodium.

A comparison of the analyses with those of other authors (Freestone and Stapleton, 1998) confirms that plant ashes (and not natron) have been used as batch materials for the fabrication of the objects.

Two fragments are made of coloured glass. The blue colour of MAO 490/40 is due to a very small cobalt addition (763 wt ppm CoO). The purple colour of MAO 490/41 is due to massive manganese oxide addition (5 wt% MnO).

3.1.2. Enamels

Table 2 shows the minimum and maximum values of various oxide contents for each type of enamels. The results can be classified either by the nature of the glass or by the colouration technique.

Two kinds of glass have been used: one with a composition similar to that of the underlying glass substrate, belonging to the class of the so-called *hard enamels*, the second one containing much higher lead oxide content (5–50 wt% PbO) called *soft enamels* because of their lower melting temperature.

Regarding the colouration techniques, a distinction must be made between *pre-fritted* and *cold ground* enamel (Brill, 2001; Freestone and Stapleton, 1998). Pre-fritted enamels are made of ground coloured glass, whereas cold ground enamels are a mixture of ground transparent glass and pigments. Although no direct observation of the enamel structures could be performed because of the absence of sampling, the knowledge of the composition allowed identifying the preparation mode.

The white enamels (Fig. 3) all contain noticeable concentration of tin oxide as whitening agent, and lead oxide. Most of them are probably pre-fritted. Yet the presence of phosphorous and of slightly higher CaO concentrations in 4 specimens may indicate a possible use of calcium phosphate as colouring agent and a possible application as cold ground enamel.

The light blue and pink enamels of MAO 490/41 and 490/35 (Fig. 3) are clearly a mixture of white enamel with a colouring agent (copper for blue, iron for pink).

Surprisingly the blue enamels never contain cobalt oxide, although cobalt is generally considered as the best and cheapest blue colouring agent for glass and ceramics. On the other hand, and by comparison with the literature (Brill, 2001; Freestone and Stapleton, 1998; Henderson, 1998), it appears that the high sulphur, potassium and alumina measured contents are typical of enamels coloured by additions of lapis lazuli or its coloured component lazurite $(\text{Na,K,Ca})_{8-x}[(\text{SO}_4,\text{S,Cl}_2)_{1-y}(\text{AlSiO}_4)_6]$. The presence of lazurite in the studied fragments was confirmed by

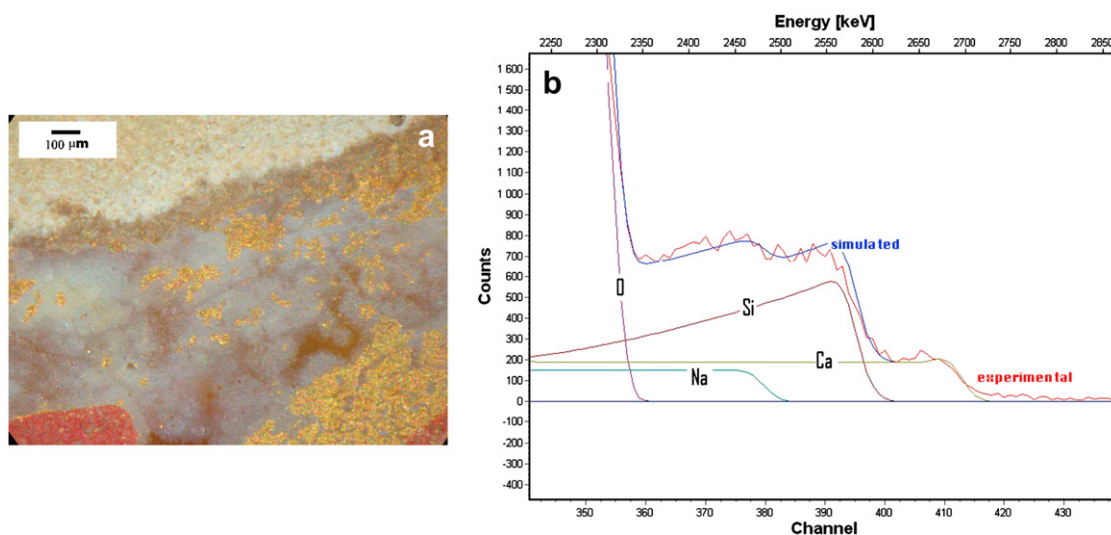


Fig. 2. Left: binocular microscope observation of an altered glass surface (specimen MAO 490/89). Right: RBS spectrum (using 3 MeV protons) and simulation profiles of the different elements by SIMNRA of an altered glass surface (specimen MAO 490/35); the RBS simulation is obtained by adding on the top of the glass with normal composition a surface layer of about 0.4 μm thickness containing no sodium.

Raman micro spectrometry (Fig. 4). This observation confirms the idea of some authors (Catalano et al., 2007; Colomban, 2003; Freestone and Stapleton, 1998) that in the geographical region of the Silk Road, difficulties of cobalt supply lead the artisans to use expensive lapis lazuli as a replacing colouring agent. The lazurite-coloured enamels belong to the category of cold ground enamels.

The red decorations are of two types: decorating red enamels (Fig. 3) or thin red lines surrounding other decorations (e.g. MAO 490/51 and 490/68 in Fig. 1). The colour is obtained by addition of haematite Fe_2O_3 , confirmed by micro-Raman analysis. Iron oxide is added to finely ground glass mixed with a tin–lead mixture. For the surrounding lines, the lead oxide and iron oxide additions are very high, allowing a high fluidity and an intense colouration.

The black enamel is coloured by addition of chromite ($\text{FeO} \cdot \text{Cr}_2\text{O}_3$) resulting in 8–9 wt% Cr_2O_3 in the enamel. Chromium is known to give enamels a viscous and grainy aspect, compensated here by high lead additions (40 wt% PbO). The black pigment has very strong colouring properties, thus black enamels do not need to be pre-fired.

Green enamels are as expected coloured by copper compounds, and probably cold ground. Cross section observations would be necessary to confirm that point.

3.2. Gilding, identification, structure, composition and thickness

Binocular and SEM observation of the gilded areas showed that they are made of gold powder (Fig. 5). Some areas have lost their gilded pattern, but, even when the decoration appears continuous and shining on naked eye, the surface fraction occupied by the powder is generally much lower than 100%.

The gold layer is in fact constituted of more or less agglomerated gold flakes with an average individual size of 10 μm (Fig. 6). Their surface fraction may be less than 50%, but on other areas they are agglomerated in larger clusters or even as nearly continuous shape. The zones between the flakes do not contain any element different from those of the underlying substrate. The flakes are always porous, and may lie either flat and parallel to the substrate surface, or in other areas strongly deformed and placed in random direction as respect to the surface.

The composition of the gold flakes has been measured by SEM-EDS analysis. The gold is pure (>99 wt%). The shape of the flakes strongly suggests that they are obtained by mechanical grinding of gold leaves (Zhao and Ning, 2000).

The thickness of the flakes is an important data because it may bring information on the gold leaf fabrication. Two methods were used to measure that thickness. The first one is RBS analysis. The

Table 2

PIXE analysis of the enamels; measured extreme contents in wt %.

	White ^a	High-lead blue	Blue	Red	Red (thin lines)	Black	Green
SiO_2	47.5–69.2	65.8–74.2	67.2–75.0	48.2–79.8	18.3–58.2	38.7	29.7–31.0
Al_2O_3	0.5–1.7	4.5–5.0	2.6–7.6	0.9–6.6	1.0–9.0	1.7	1.2–1.6
Fe_2O_3	0.3–0.7	0.3–1.0	0.4–0.7	2.7–15.4	7.5–23.6	2.8	0.4–0.5
MnO	0.2–0.8	0.4–0.6	0.1–1.2	0.2–1.7	0.3–1.7	0.3	<0.1
MgO	1.1–3.1	1.7–3.3	1.4–3.9	0.8–4.1	0.5–2.5	2.4	0.5–1.2
CaO	4.7–9.5	6.2–9.7	5.0–9.8	1.9–13.0	1.8–10.0	2.4	1.4–2.9
Na_2O^b	0.9–8.1	3.0–8.3	3.2–6.4	1.8–7.1	1.5–6.1	3.0	1.1–1.9
K_2O	1.4–2.8	2.4–3.5	2.2–3.8	2.1–3.6	1.0–4.1	1.5	1.1–1.3
CuO	<0.1	<0.1	<0.1	<0.1	0–0.5	1.2	1.2–2.0
SnO_2	6.5–12.9	8.0–9.0	–	0–6.5	0–2.1	–	6.9–9.1
PbO	2.2–17.2	5.0–12.4	0–1.5	0–8.4	3.8–69.1	41.8	46.3–47.5
Cl	0.6–1.2	0.7–2.4	0.6–1.1	0.6–2.2	0–1.8	0.7	1.2–1.9
SO_3	0–1.8	1.1–2.0	0.9–4.2	0–4.1	0–10.6	–	–
P_2O_5	0–2.8	0–0.4	0–0.2	0–2.1	0–2.9	–	–
Cr_2O_3	–	–	–	–	–	8.7	–

^a Pink and pale blue enamels have a composition similar to the white enamels with $\text{CuO} = 1.2$ for the blue enamel and $\text{Fe}_2\text{O}_3 = 0.8$ for the pink enamel.

^b No PIXE control analysis.

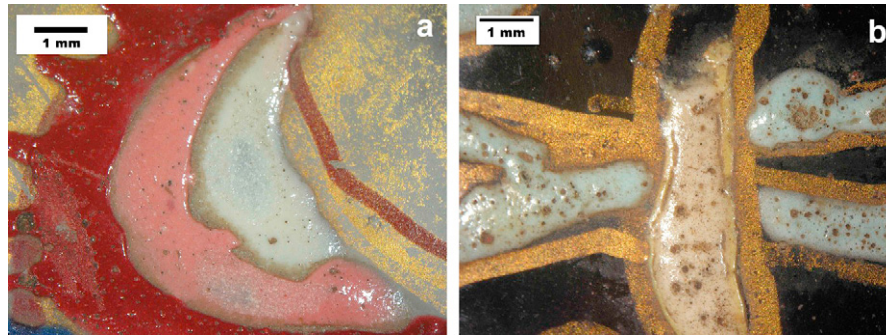


Fig. 3. White, pink, light blue and red enamels observed in binocular microscope. Left MAO 490/35; right MAO 490/41.

interpretation of the spectra is difficult, as the incident ion beam is larger than the average size of the flakes, and the flakes themselves are porous and not flat. Indeed the SIMNRA code used for RBS spectra simulation (Mayer, 1997) is based on the hypothesis of uniformly stacked layers of constant composition and thickness, which is not the case here. The simulated thicknesses are thus over estimated. A rough estimation of the foil thickness by RBS spectra simulation is found smaller than 500–600 nm.

The second method is based on a computation model in SEM-EDS microanalysis, where the measurement can be performed on a microscopic area smaller than the flakes size. The computation code used is the STRATAGEM code developed for thin foils stratigraphic analysis in electron probe microanalysis (Pouchou, 2002). The gold signal yield is measured on a given point and normalised to the signal expected from a bulk gold specimen in the same conditions (“k-ratio”). Knowing the composition of the gold-free silicate substrate the computation code gives an estimation of the gold thickness (Fig. 7). The average results obtained on a large number of areas range between 100 and 300 nm. They may be distorted by the “skirting effect” described above (§ 2.2.), which increases the relative signals from the substrate and thus leads to an underestimation of the gold foil thickness. An estimation of that effect by measurements on known standards shows that the induced error is not larger than 10–20 nm.

Combining the results of the two methods, the gold leaf used to obtain the flakes is between 150 and 300 nm thick. This thickness is characteristic of beaten gold. A recent investigation on gilded

Islamic ceramics has shown that the use of beaten gold leaves of a few hundreds nanometres thick was already known at the considered period (Pacheco, 2007) in the Islamic world.

3.3. The gold–glass interface, alteration

The fragment areas where gold decoration has disappeared were carefully observed in optical microscopy and revealed an unexpected roughness (Fig. 8) which has the same aspect than frosted glass. This aspect could be observed on all the fragments.

The roughness was measured by optical micro topography (Fig. 9). The mean roughness is about 1 μm , whereas the neighbouring areas have a roughness smaller than 200 nm. The lateral wavelength of roughening is regular and less than 10 μm .

At the SEM scale (Fig. 10) the previously gilded areas also show micrometric bubbles. The size and periodic occurrence of these bubbles seem larger than those of the mentioned roughness.

All these observations will be commented in the following part with the discussion on gliding process and adhesion mechanisms.

4. Discussion

4.1. The fabrication process

For 9 out of 12 objects, the results tend to confirm the general decorative process partially described by some authors (Freestone, 2002; Freestone and Stapleton, 1998) (Fig. 11):

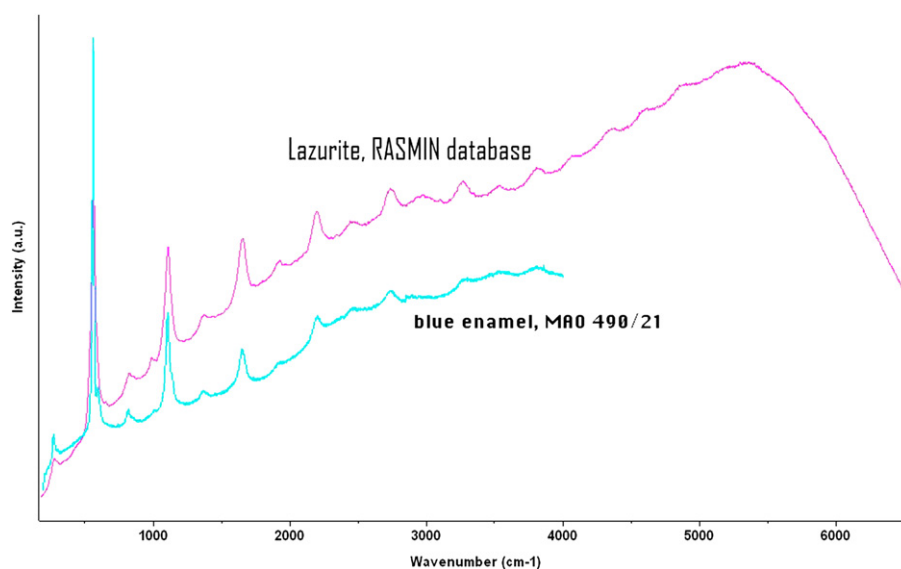


Fig. 4. Raman spectrum of lazurite from the RASMIN database and micro-Raman spectrum from the blue enamel of MAO 490/21.

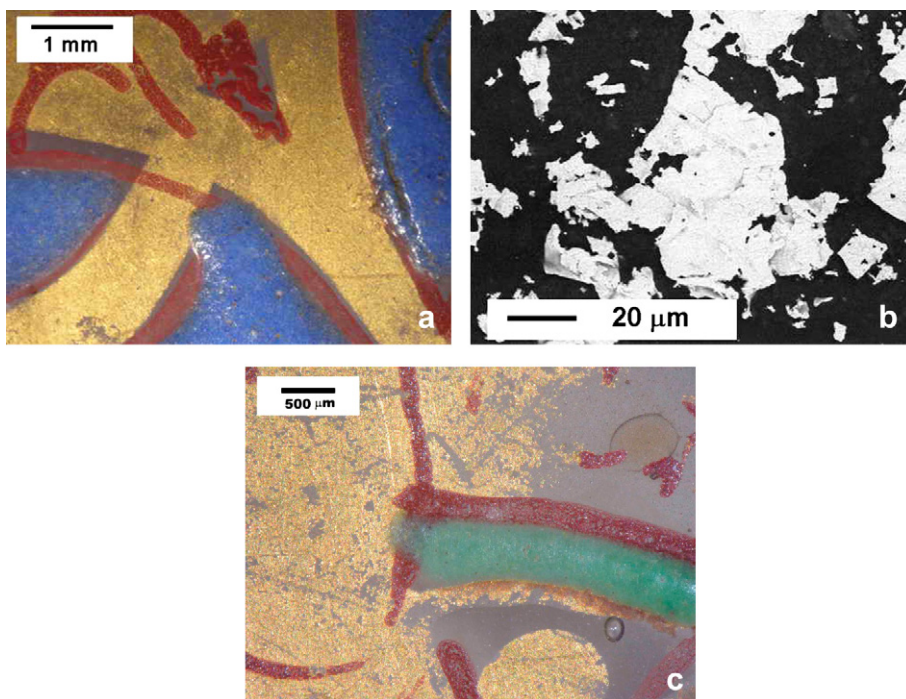


Fig. 5. Binocular observation (left and right) and SEM observation (centre) of gilded areas.

- The gilding mixture, constituted of gold flakes finely ground from beaten gold leaves mixed with an organic binder (gum Arabic?) is applied with a brush on the already shaped glass object body following a previously defined design;
- The design is sometimes surrounded by a fine line of red enamelling mixture of the second type described in § 3.1.2, rich in lead and iron oxide;
- The other enamelling mixtures of various colours are then applied to complete the decoration;
- The object is fired at a temperature high enough to provoke the formation of the enamels and adhesion of the gold flakes to the

substrate, but low enough to avoid too much softening of the body.

The question of the number and temperature of firings is still open. As stated in the results part, the composition of the glass constituting the enamels may be either not very different from that of the glass body or noticeably different, e.g. when the lead content is high (surrounding red, white, black, green and light blue). This means that the melting temperatures of the enamels may be very different from each other. On the other hand, the presence on the objects of only two marks of pontil fastening (a pontil is a stick used

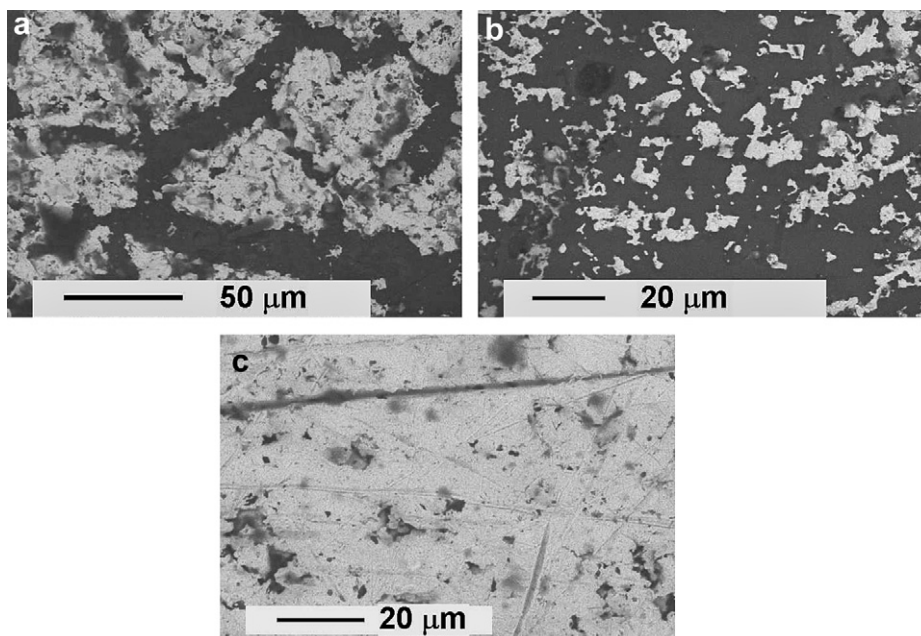


Fig. 6. Various gilding powder surface density, as observed by SEM.

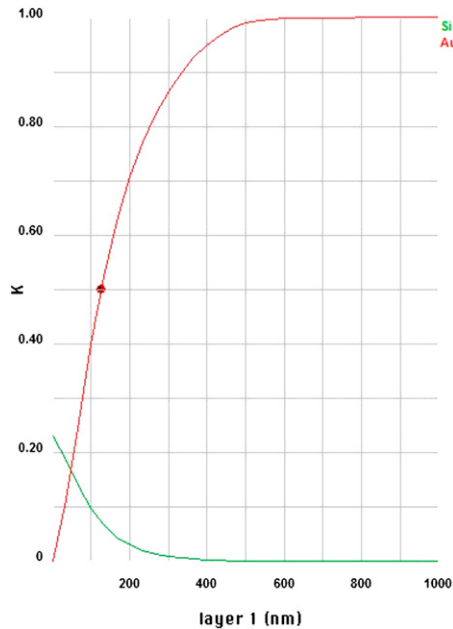


Fig. 7. k-Ratio value for the $M\alpha$ X-ray line of gold (ratio between the line intensity of the specimen and the line intensity of a gold standard) as a function of the gold layer thickness on a glass substrate, as computed by the STRATAGEM code. The point corresponding to a gold k-ratio of 0.5 corresponds to a gold layer of 120 nm thickness.

by glassmakers to introduce an object into the firing furnace) tends to show that the decoration firing was probably done in one step: one pontil for the object body forming, the second for its decoration (Carboni, 2001b). This means that the decoration firing is done at a temperature very near, if not over, the softening temperature of the body, i.e. above 500 °C and below 800 °C. The decoration firing has to be as short as possible in order to avoid a too large deformation of the objects (Freestone and Stapleton, 1998). The irregular

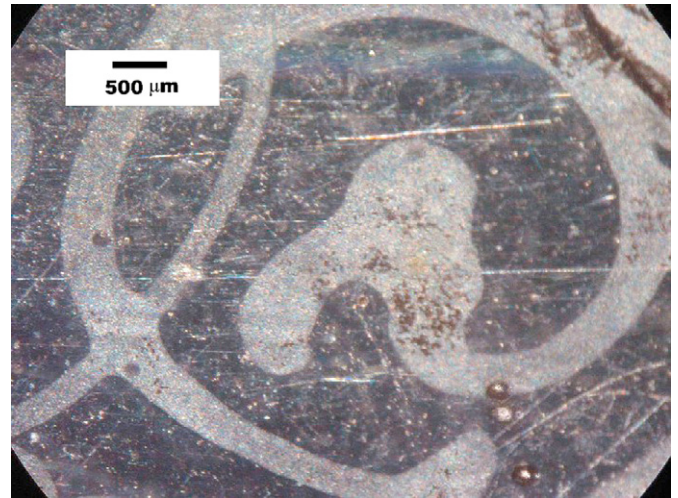


Fig. 8. Binocular observation in transmitted light of previously gilded arabesques of MAO 490/21 fragment.

aspect of some cold ground observed enamels (Fig. 12) is an argument for the occurrence of such a short firing duration.

Three objects show an aspect different from the others (MAO 490/20, MAO 490/34 and MAO 490/89, Fig. 1). For these objects, the fabrication process is obviously different (Fig. 13). Gold is not applied on the glass but on a red enamel background. It is probable that that enamel was fired before the application of the gilding mixture. In that case two firing steps were necessary for the decoration.

4.2. Gold application and adhesion

As stated previously, the gold decorations are made of gold flakes mixed with an organic binder. Those flakes result from the

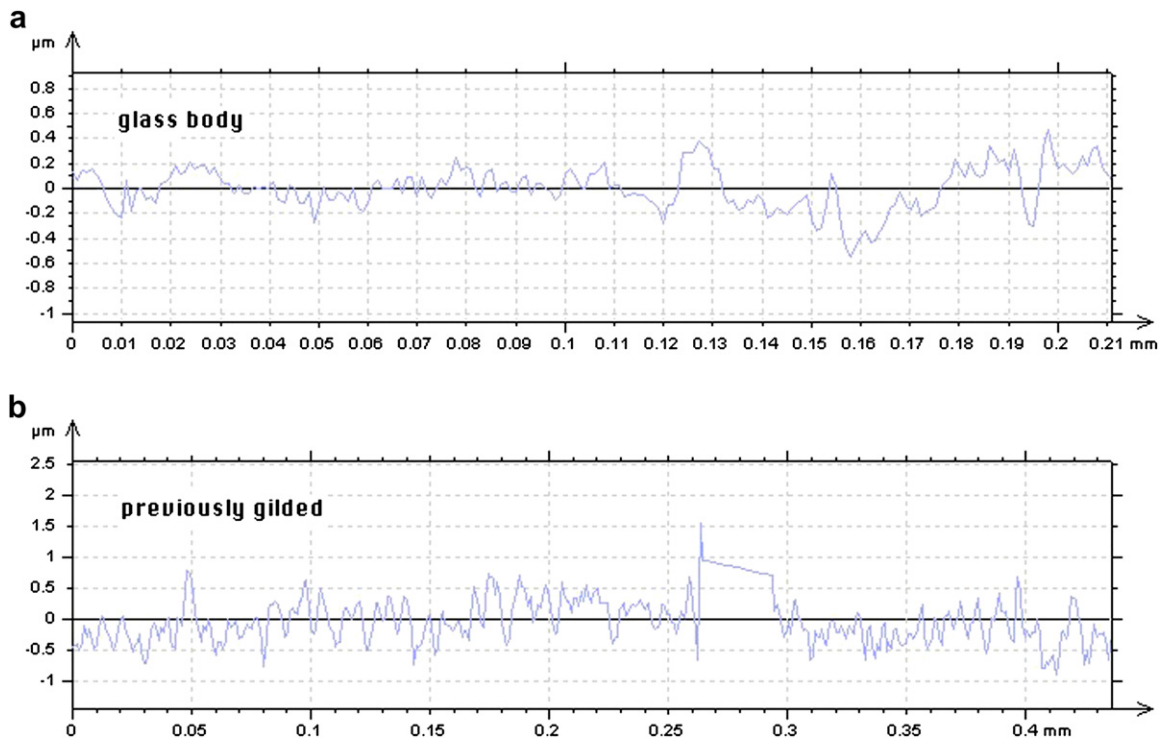


Fig. 9. Topographic profile measured in the previously gilded area (b), compared to the profile on the glass substrate (a). Note the different scales for abscissa and ordinate. The anomaly at 0.27–0.29 mm of profile b is an artefact due to a dust particle.

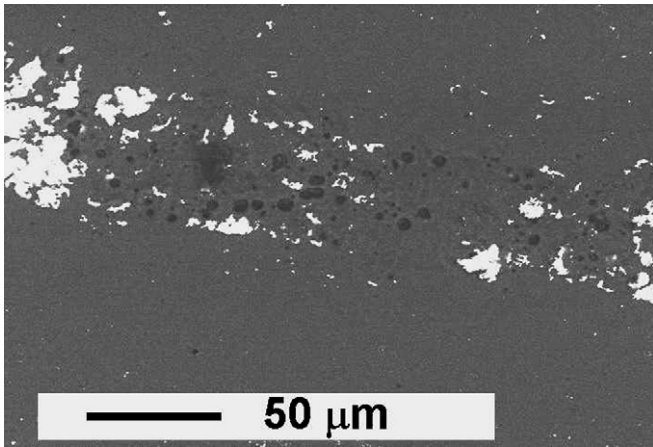


Fig. 10. Surface SEM observation of a gilded area partially unglilded. The white zones are gold flakes; black spots are micro bubbles.

mechanical grinding of very thin pure gold leaves. The firing temperature discussed above is evidently high enough to allow a complete decomposition of the organic binder and a degassing of the glass, leading to the formation of the bubbles observed at the interface (Fig. 10). The adhesion of gold to glass may be explained by the mechanism proposed in a recent study on modern “liquid” gold decoration of glass (Darque-Ceretti et al., 2008): gold diffuses into glass on a short distance (200 nm), and sodium diffuses out on the same distance, leading to the formation of a limited thickness of modified glass containing some quantities of gold aggregates. The mechanism of gold diffusion (atomic or ionic) and agglomeration as nano-aggregates is not clarified yet. This hypothesis of a contribution of inward gold diffusion is strengthened by an important observation (Fig. 14): RBS analysis performed on a previously gilded surface clearly revealed the presence of a very small quantity of



Fig. 12. White cold ground enamel of MAO 490/41. Irregular aspect with bubbles and cracks probably due to a very short firing.

gold (9×10^{15} at.cm⁻², i.e. about 6 atomic layer equivalent) whereas no gold was visible in microscopy.

The final aspect of the gilded decoration depends on the density (flakes content) of the gilding mixture when it is applied. The micrographs of Fig. 6 show that that density may vary in large proportions, even on the same object. The decoration may have been burnished to improve the final aspect of the objects (Fig. 15).

4.3. Surface roughening of the previously gilded areas

The particular surface feature observed on the areas where gold decoration has disappeared (Figs. 8 and 9) may have different origins. Are the observed roughness and the micro bubbles normal features of the gold/glass interface, or do they result from the alteration of that interface? Fortunately, it was possible to observe

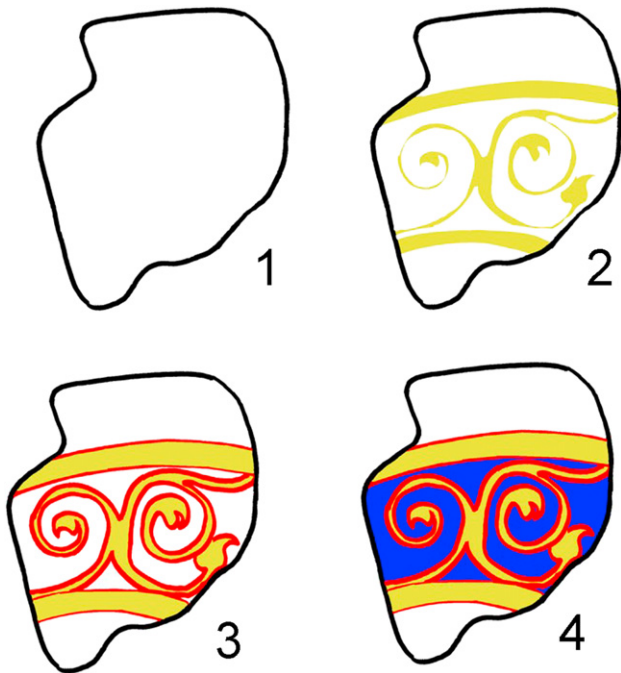


Fig. 11. Decoration steps of enamelled and gilded glass artefacts. Gilding mixture application (2); application of the red surrounding enamel (3); application of enamels (4); final firing.

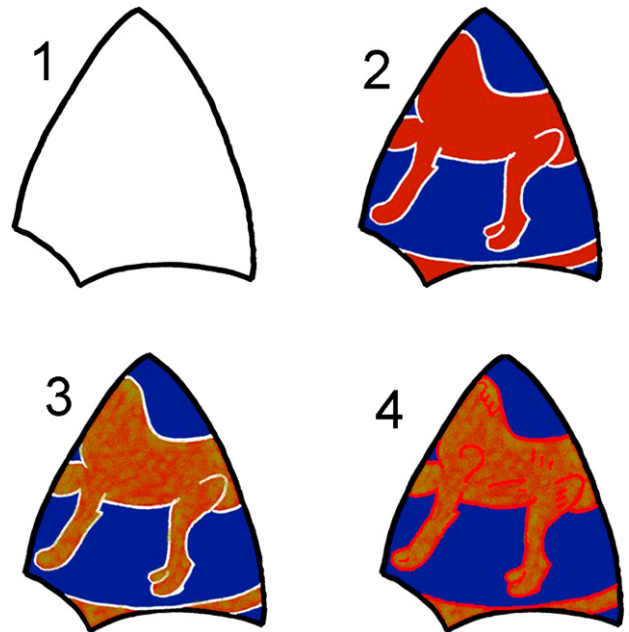


Fig. 13. Decoration steps for MAO 490/20, MAO 490/34 and MAO 490/89 fragments: application and firing of enamel on the glass substrate (2); application of the gilding mixture (3); application of the surrounding red enamel (4); final firing.

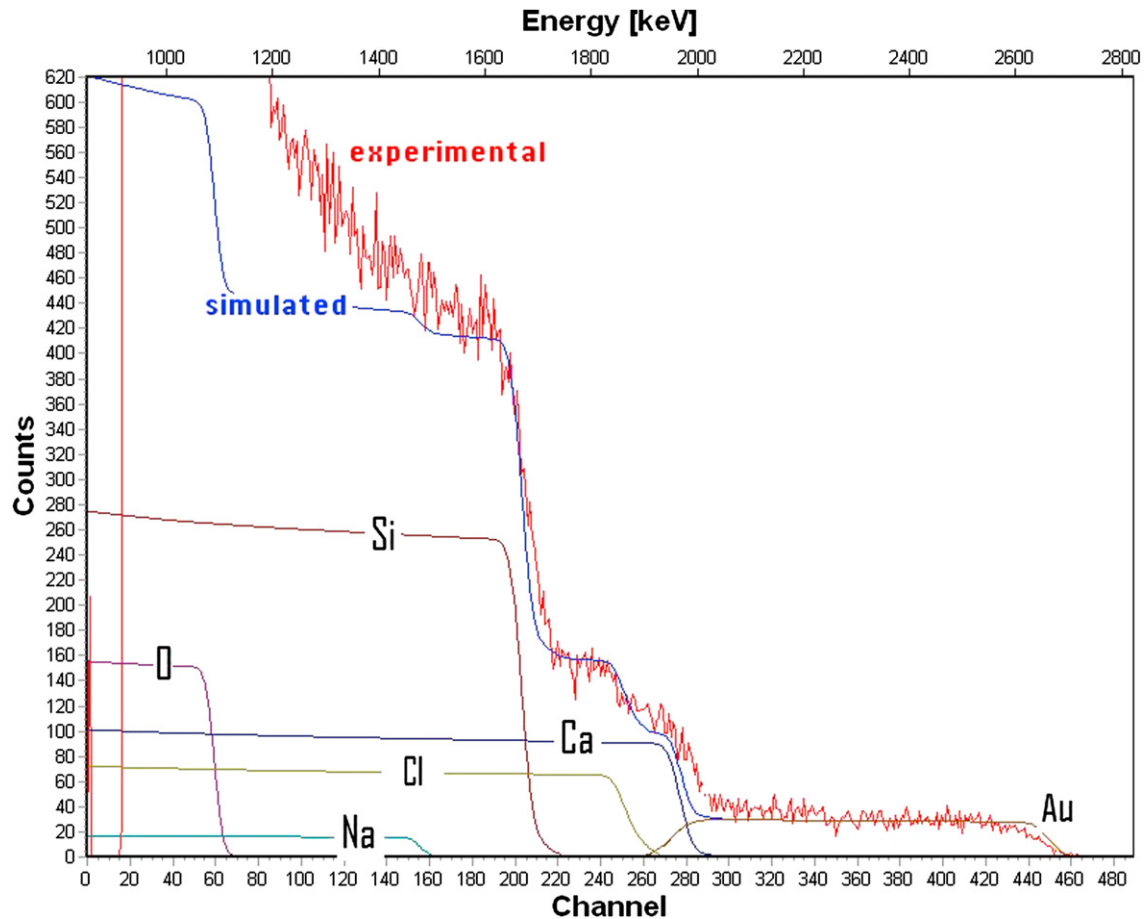


Fig. 14. RBS spectrum on a previously gilded area of MAO 490/21 showing the presence of a surface layer containing 9×10^{15} at.cm⁻² gold. The noisy curve is the experimental RBS spectrum. Other curves are the simulated elemental spectra. The presence of surface gold is attested by the “gold” curve.

in the SEM the edge of a specimen, where the gold decoration appears covered by the neighbouring enamel (Fig. 16). This occurrence is rare, because, as discussed earlier, the artisan used to apply the gilding mixture on well defined areas before applying the enamel to other areas. On the micrographs of Fig. 16, the gold flakes alignment defines the position of the substrate/gilding/enamel interface. Two observations can be done: first, bubbles are indeed present at that interface, separated by distances larger than several

tens of μm ; second the gold/glass interface appears not well defined and the gold flakes are not precisely lying parallel to the interface.

It was unfortunately impossible to increase the magnification enough to observe a possible roughness of the interface of the order of that measured at the surface of the ungilded areas.

The zones of the glass substrate which were intended to be gilded might have been intentionally roughened by the artisan in order to ensure a better adhesion of the gold flakes after application and firing. The absence of chemical frosting procedure at this time makes this hypothesis unlikely. The frosting would have to be manual and would appear less regular and probably rougher.

Another hypothesis is that the fine roughening is a consequence of the firing of the glass. As discussed earlier, the temperature of firing is probably higher than the softening temperature of the substrate. The degassing of the surface could induce micro bubbles and thus the micro roughening of the interface.

It was impossible to know if the gold/glass interface of the objects is already roughened in the preserved gilded region, because no sampling was allowed. Some larger bubbles were observed in the particular case reported in Fig. 16. Possible occurrence of smaller and more regular defects is not to be ruled out.

A third hypothesis is that the roughening is a consequence of the weathering of the interface. A recent study (Darque-Ceretti et al., 2008) showed that ageing of the glass/gold interface occurs by a cohesive rupture inside the fine layer of glass modified by gold diffusion under the gold deposit. The presence of small quantities of gold near the surface of the ungilded areas (Fig. 14) is an argument for such a degradation mechanism.

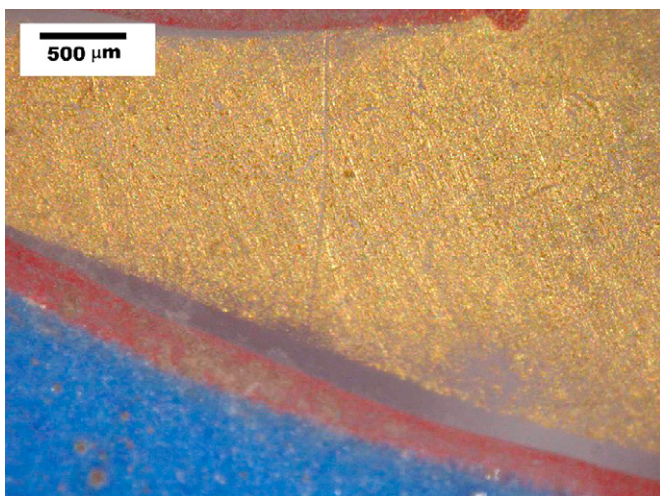


Fig. 15. Gilding probably burnished after application and firing, MAO 490/51.

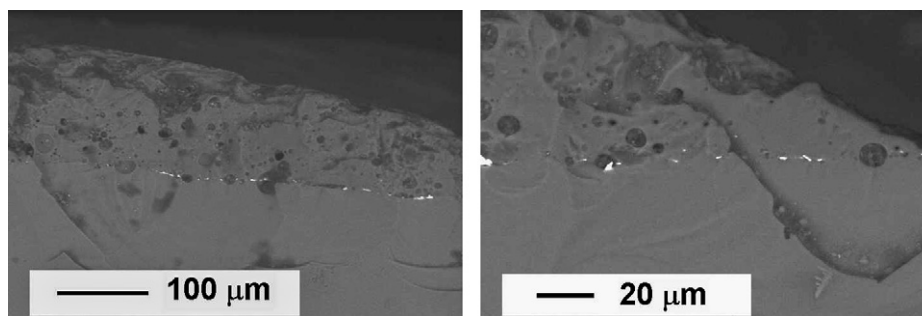


Fig. 16. SEM observations at two magnifications of the edge of MAO 490/41. The white spots are gold flakes, the black zones are bubbles.

None of these hypotheses can be validated yet. Laboratory experiments using various binders and firing temperature would be necessary to a further understanding of the formation of the surface micro roughness.

5. Conclusions

This study of a selected set of Islamic enamelled and gilded glass artefacts manufactured in Egypt or Syria during the Ayyubid or Mamluk period (13th–14th centuries) confirms existing data on the enamelling process used by the glassware craftsmen. More importantly it brings new information on the materials and technique and mechanisms of the gilding process.

As expected the glass bodies are plant-ash based soda-lime-silica glass.

Enamels are of the two usual types: pre-fired enamels and cold ground enamels. Colourations are obtained by usual pigment additions: tin and lead for white, iron oxide for red, copper for green, chromite (plus lead) for black. The case of the blue colouration is particular: very small cobalt addition is used for occasional colouration of the body, but blue enamel is obtained by addition of lapis lazuli rather than cobalt, perhaps for commercial reason. The presence of such an expensive pigment shows the importance and commercial value of those artefacts.

The comprehensive non-destructive study of the gilded decoration brings important results. The gilding mixture is made from ground thin (150–300 nm) beaten gold leaves and applied, for most of the objects (9 out of 12) on the glass body directly. Adhesion of the gold flakes results from an atomic diffusion of gold into the glass. For these 9 objects, the decoration firing was probably performed in one step, after application of the gilding and enamelling mixtures. The firing temperature was higher than the glass substrate softening temperature and the firing step should have been rapid to avoid deformation of the artefact body. For the other 3 objects, the decoration application and firing was done in two steps: application and firing of a background enamel, then application of the gilding mixture and of the surrounding red lines, followed by a second firing.

Laboratory experiments would be necessary to precisely identify the adhesion mechanism and to understand the weathering mechanism of the gilded decoration, particularly the reason of occurrence of the fine roughness observed on the previously gilded areas.

Acknowledgments

That study was initiated as part of the ANR program “DORAI”, directed by Remy Chapouliè, from the Centre de Recherche de Physique Appliquée à l’Archéologie (CRPAA-IRAMAT, UMR CNRS 5060, Bordeaux 3 University). The artefacts were chosen in collaboration with Claire Pacheco, DORAI PhD, and kindly supplied by Mrs Sophie Makariou, Curator in Chief and Carine Juvin,

engineer of the Department of Islamic Arts (DAI) of the Louvre museum. IBA were done with help of the AGLAE accelerator team (Joseph Salomon[†] and Laurent Pichon). STRATAGEM code simulation was obtained thanks to the kind collaboration of Patrice Lehuédé and the access to Saint Gobain Research laboratory.

References

- Allan, J.W., 1973. Abu'l-Qasim treatise on ceramics. Iran 11, 111–120.
- d’Avennes, P., 1877. L’Art arabe, d’après les monuments du Caire. L’Aventurine, Paris.
- Brill, R.H., 2001. Some thoughts on the chemistry and technology of Islamic glass. In: Carboni, S., Whitehouse, D. (Eds.), Glass of the Sultans. Metropolitan Museum of Art, New York, pp. 25–45.
- Calligaro, T., Dran, J.-C., Salomon, J., 2004. Ion beam microanalysis. In: Janssens, K., Van Grieken, R. (Eds.), Non-destructive Microanalysis of Cultural Heritage Materials. Elsevier, Amsterdam, pp. 227–276.
- Catalano, I.M., Genga, A., Laganara, C., Laviano, R., Mangone, A., Marano, D., Traini, A., 2007. Lapis lazuli usage for blue decoration of polychrome painted glazed pottery: a recurrent technology during the Middle Ages in Apulia (Southern Italy). Journal of Archaeological Science 34, 305–511.
- Carboni, S., 2001a. Glass production in the Islamic world: a historical overview. In: Carboni, S., Whitehouse, D. (Eds.), Glass of the Sultans. Metropolitan Museum of Art, New York, pp. 3–7.
- Carboni, S., 2001b. Painted glass. In: Carboni, S., Whitehouse, D. (Eds.), Glass of the Sultans. Metropolitan Museum of Art, New York, pp. 199–274.
- Carboni, S., 2003. Mamluk Enamelled and Gilded Glass in the Museum of Islamic Art Qatar. Islamic Art Society, London.
- Carboni, S., Whitehouse, D., 2001. Glass of the Sultans. Metropolitan Museum of Art, New York.
- Carlton, R.A., Lyman, C.A., Roberts, J.E., 2004. Accuracy and precision of quantitative energy-dispersive X-ray spectrometry in the environmental scanning electron microscope. Scanning 26, 167–174.
- Colomban, P., 2003. Lapis lazuli as unexpected blue pigment in Iranian Lâjvardina ceramics. Journal of Raman Spectroscopy 34, 420–423.
- Darque-Ceretti, E., Aucouturier, M., Deram, V., 2002. An investigation of gold/ceramic and gold/glass interfaces. Gold Bulletin 35, 118–129.
- Darque-Ceretti, E., Deram, V., Aucouturier, M., 2008. Organometallic based gold decoration, formation and durability. Surface Engineering 24, 103–112.
- Darque-Ceretti, E., Aucouturier, M., 2007. The surface of cultural heritage artefacts: physicochemical investigations for their knowledge and their conservation. Chemical Society Reviews 36, 1605–1621.
- du Pasquier, J., 2005. Histoire du verre: le Moyen-Âge. Masson, Paris.
- Ezrati, J.J., Bouquillon, A., Vigears, D., Bormand, M., Meyohas, M.-E., 2007. La microtopographie pour une meilleure connaissance des oeuvres. Contrôles, Essais, Mesures 21, 32–33.
- Freestone, I., Stapleton, C., 1998. Composition and technology of Islamic enamelled glass of the thirteenth and fourteenth centuries. In: Ward, R. (Ed.), Gilded and Enamelled Glass from the Middle-East. The British Museum, London, pp. 122–128.
- Freestone, I., 2002. The relationship between enamelling on ceramics and on glass in the Islamic world. Archaeometry 44, 251–255.
- Gudenrath, W., 2001. A survey of Islamic glassworking and glass-decorating techniques. In: Carboni, S., Whitehouse, D. (Eds.), Glass of the Sultans. Metropolitan Museum of Art, New York, pp. 46–70.
- Henderson, J., 1998. Blue and other translucent glass decorated with enamels: possible evidence for trade in cobalt-blue colourants. In: Ward, R. (Ed.), Gilded and Enamelled Glass from the Middle-East. The British Museum, London, pp. 116–121.
- Lamm, C.J., 1941. Oriental Glass of Medieval Date found in Sweden and the Early History of Lustre-Painting. Kungl. Vitters Hist. och Antikvitets Akad., Stockholm.
- Maxwell, J.A., Campbell, J.L., Teesdale, W.J., 1988. The Guelph PIXE software package. Nuclear Instruments and Methods in Physics Research B43, 218–230.
- Mayer, M., 1997. ‘SIMNRA, ©Max Planck-Institut für Metallphysik’. Available from: www.rzg.mpg.de/~mam/.

- Pacheco, C., 2007. Etude de films d'or sur matière vitreuse. Application à la céramique glaçurée islamique médiévale. Asie centrale XI^e-XV^e s.- Iran XII^e-XIII^e s. PhD Thesis, Université Michel de Montaigne, Bordeaux 3.
- Pouchou, J.L., 2002. X-ray microanalysis of thin surface films and coatings. *Mikrochimica Acta* 138, 133–152.
- Schmoranz, G., 1899. Old Oriental gilt and enameled Glass Vessels. Extant in Public Museums and Private Collections, London.
- Tesmer, J.R., Nastasi, M., 1995. Handbook of Modern Ion Beam Materials Analysis. Materials Research Society.
- Théophilus, 2000. Essai sur divers arts: recettes pratiques de l'enluminure, l'orfèvrerie, l'ivoire, le vitrail, la fresque, et autres arts. Clermont-Ferrand, Paleo.
- Verità, M., 1998. Analyses of early enamelled glass in nineteenth century collections. In: Ward, R. (Ed.), Gilded and Enamelled Glass from the Middle-East. The British Museum, London, pp. 129–134.
- Ward, R., 1998. Gilded and Enamelled Glass from the Middle-East. The British Museum, London.
- Zhao, H., Ning, Y., 2000. Techniques used for the preparation and application of gold powder in ancient China. *Gold Bulletin* 33, 103–105.